

Proceedings Article

Hands-free Reconstruction for MPI

Konrad Scheffler ^{a,b,*}, Marija Boberg ^{a,b}, Tobias Knopp ^{a,b}

^aSection for Biomedical Imaging, University Medical Center Hamburg-Eppendorf, Hamburg, Germany

^bInstitute for Biomedical Imaging, Hamburg University of Technology, Hamburg, Germany

*Corresponding author, email: ko.scheffler@uke.de

© 2023 Scheffler *et al.*; licensee Infinite Science Publishing GmbH

This is an Open Access article distributed under the terms of the Creative Commons Attribution License (<http://creativecommons.org/licenses/by/4.0>), which permits unrestricted use, distribution, and reproduction in any medium, provided the original work is properly cited.

Abstract

In iterative system-matrix-based reconstruction in Magnetic Particle Imaging, three major parameters control the amount of regularization. Finding the right choice for these parameters is commonly done by user input and requires time and experience. We propose a method that enables automatic reconstruction and achieves good results on a measured concentration series.

I. Introduction

The imaging equation in Magnetic Particle Imaging (MPI) describing the connection between particle distribution and voltage signal poses an inverse problem in the frequency domain based on a measured system matrix [1, 2]. Considering a regularized least squares approach, this is commonly solved using iterative solvers, e.g. the regularized Kaczmarz method [3]. The quality of the reconstructed image mainly depends on three parameters: the weighting of the regularization term, the frequency selection of the voltage signal and the number of total iterations [4]. Having a clear measurement with high signal-to-noise ratio (SNR) over all frequency components, good results can be achieved with weak regularization and by considering the vast majority of frequency components. For a noisy measurement the regularization needs to be stronger and frequencies with a bad SNR need to be excluded from the reconstruction process. Thus, the reconstruction parameters depend not only on the measurement settings but also on the shape of the phantom and the iron concentration. Finding an ideal choice of the parameters for each measurement remains a major challenge in MPI reconstruction. Algorithms for finding a good regularization strength [5], as well as a good SNR-threshold [6] have been proposed, but the state of the art procedure is up to now trial and

error supported by experience. In this work, we present a method, that enables automatic reconstruction without user input by adapting the SNR threshold and regularization parameter in each iteration of the solver and defining a proper stopping criterion. The method is validated on the dot-phantom of the MPI concentration study published in [4].

II. Methods and materials

The discrete MPI imaging equation in matrix-vector form is given by

$$\mathbf{u}_{\text{meas}} = \mathbf{S}\mathbf{c}, \quad (1)$$

where $\mathbf{c} \in \mathbb{R}_+^N$ is the particle concentration vector, $\mathbf{S} \in \mathbb{C}^{K \times N}$ is the system matrix and $\mathbf{u}_{\text{meas}} = \mathbf{u} + \boldsymbol{\eta}$ with $\mathbf{u}, \boldsymbol{\eta} \in \mathbb{C}^K$ is the measured voltage vector with additive background noise. $N, K \in \mathbb{N}$ are the total number of sampling positions and Fourier coefficients, respectively. Solving (1) for the particle concentration vector is commonly done by applying an iterative solver to the Tikhonov regularized least squares problem

$$\mathbf{c}_\lambda = \underset{\mathbf{c} \in \mathbb{R}_+^N}{\operatorname{argmin}} \|\mathbf{S}\mathbf{c} - \mathbf{u}_{\text{meas}}\|_2^2 + \lambda \|\mathbf{c}\|_2^2, \quad (2)$$

with the parameter $\lambda \in \mathbb{R}_+$ controlling the amount of regularization. Bigger values for λ lead to a stronger regularization. As described in [4], noise amplification is further regulated by removing frequencies with low SNR values from the linear system. To this end, an SNR-threshold $\Theta \in \mathbb{R}_+$ is introduced, such that only frequency components with $\text{SNR}_k > \Theta$ for $k \in \{1, \dots, K\}$ are considered for reconstruction. A higher threshold Θ leads to stronger regularization. Note that because of the distribution of high-SNR frequencies around higher harmonics of the MPI-scanners excitation frequency [7] the connection between Θ and the number of rows in the linear system is not linear. The third control of regularization is the number of iterations $\iota \in \mathbb{N}$ for iterative solvers. A lower number of iterations is equivalent to a stronger regularization. Altogether, we collect the three reconstruction parameters in a set

$$\mathcal{P} := (\lambda, \Theta, \iota). \quad (3)$$

To achieve an automated reconstruction, the goal is to condense the parameter-triplet \mathcal{P} into a single parameter. To this end, we map the regularization strength λ and the SNR threshold Θ to ι , such that each iteration has different but predefined values for λ and Θ . The idea is, that the first iterations work only on few frequencies with a strong regularization (high Θ and λ) and later iterations include more frequencies with a dwindling regularization term (low Θ and λ) for a better resolution. In between should be a steady and smooth transition with polynomial decrease, which can be described by functions of the form

$$h_j(x) = \frac{\alpha_j}{1 + (\beta_j x - \beta_j)^{\gamma_j}}, \quad (4)$$

for $1 \leq x \in \mathbb{R}$, $\alpha_j, \beta_j, \gamma_j \in \mathbb{R}_+$. The index $j \in \{\Theta, \lambda\}$ associates h to the respective regularization parameter. A further regulation is a minimum value $\Theta_{\min} \geq 1$, preventing the inclusion of pure noise frequencies. The values of α_Θ and Θ_{\min} are dependent on the receive path of an MPI scanner and thus have to be adjusted for different receive coils.

The second step is to find a suitable stopping criterion for the iterative solver. When using the regularized Kaczmarz method, the auxiliary vector converges to the scaled residual $-\lambda^{-\frac{1}{2}}(\mathbf{S}\mathbf{c} - \mathbf{u}_{\text{meas}})$. This can be exploited to calculate the L-curve between the 2-norms of the residuum and \mathbf{c} . However, typical L-curve stopping criteria based on the curvature of the L-curve [5] do not take into account the change in system size and regularization in each iteration. Thus, it is important to normalize the residual-norm with respect to the amount of considered frequencies in each iteration. To further stabilize the criterion it is meaningful that the curvature $\Psi \in \mathbb{R}$ should exceed a certain level dependent on the size of the solution norm, giving the final stop criterion at iteration

Table 1: Error-Results

conc. (mmol/l)	hands-free		hands-on	
	NRMSD	iter.	NRMSD	\mathcal{P}
400	1.48e-2	20	1.12e-2	(2e-4,1.6,14)
200	1.5e-2	18	1.03e-2	(2e-3,1.3,26)
100	1.67e-2	16	1.06e-2	(3e-3,1.4,26)
50	1.88e-2	14	1.11e-2	(5e-3,1.7,26)
25	2.63e-2	10	1.48e-2	(0.01,1.8,22)
12.5	2.99e-2	9	1.70e-2	(0.04,2.7,10)
6.25	3.92e-2	7	2.04e-2	(0.06,3,1)
3.13	5.37e-2	3	2.39e-2	(0.09,4,1)
1.56	5.59e-2	4	3.93e-2	(0.2,10,1)
0.78	6.84e-2	2	5.84e-2	(0.6,30,1)
0.39	9.42e-2	2	0.110	(1,30,1)
0.2	0.118	2	0.146	(5.5,70,1)

$i \in \mathbb{N}$ by

$$\frac{\Psi_i}{\|\mathbf{c}_1\|_2} > \delta \wedge \frac{\Psi_i}{\Psi_{i-1}} > \varepsilon, \quad (5)$$

for $\delta, \varepsilon \in \mathbb{R}_+$.

III. Experiments

We evaluated the described method on the concentration study with a single-dot phantom described in [4], measured with the preclinical MPI system 25/20FF (Bruker Corporation, Ettlingen, Germany). It consists of a series of 12 measurements where the iron concentration is halved for each new measurement starting with $\kappa_1 = 400$ mmol/l. The parameters for the mapping functions and the stop criterion were chosen as $\alpha_\lambda = 5, \beta_\lambda = 0.2, \gamma_\lambda = 5, \alpha_\Theta = 60, \beta_\Theta = 0.28, \gamma_\Theta = 2, \Theta_{\min} = 1.3, \delta = \frac{1}{4}, \varepsilon = 2$. We use normalized values for λ using the nuclear norm of the system matrix. For an error-analysis we voxelized a ground-truth out of the CAD files of the dot phantom and use the normalized root mean square deviation (NRMSD) between the calculated concentration vectors and the ground-truth phantom. Furthermore, we carefully chose reconstruction parameters by hand to establish a reference reconstruction.

IV. Results

The number of iterations to satisfy the stopping criterion is given for each concentration in Table 1. Furthermore the optimal parameter set resulting from the hand-tuned reconstruction as well as the NRMSD values are reported. The corresponding reconstruction results are plotted in Fig. 1, using a maximum intensity projection in z -direction (xy -plane). It can be seen, that the hands-free reconstruction is able to adapt ι and thus the amount

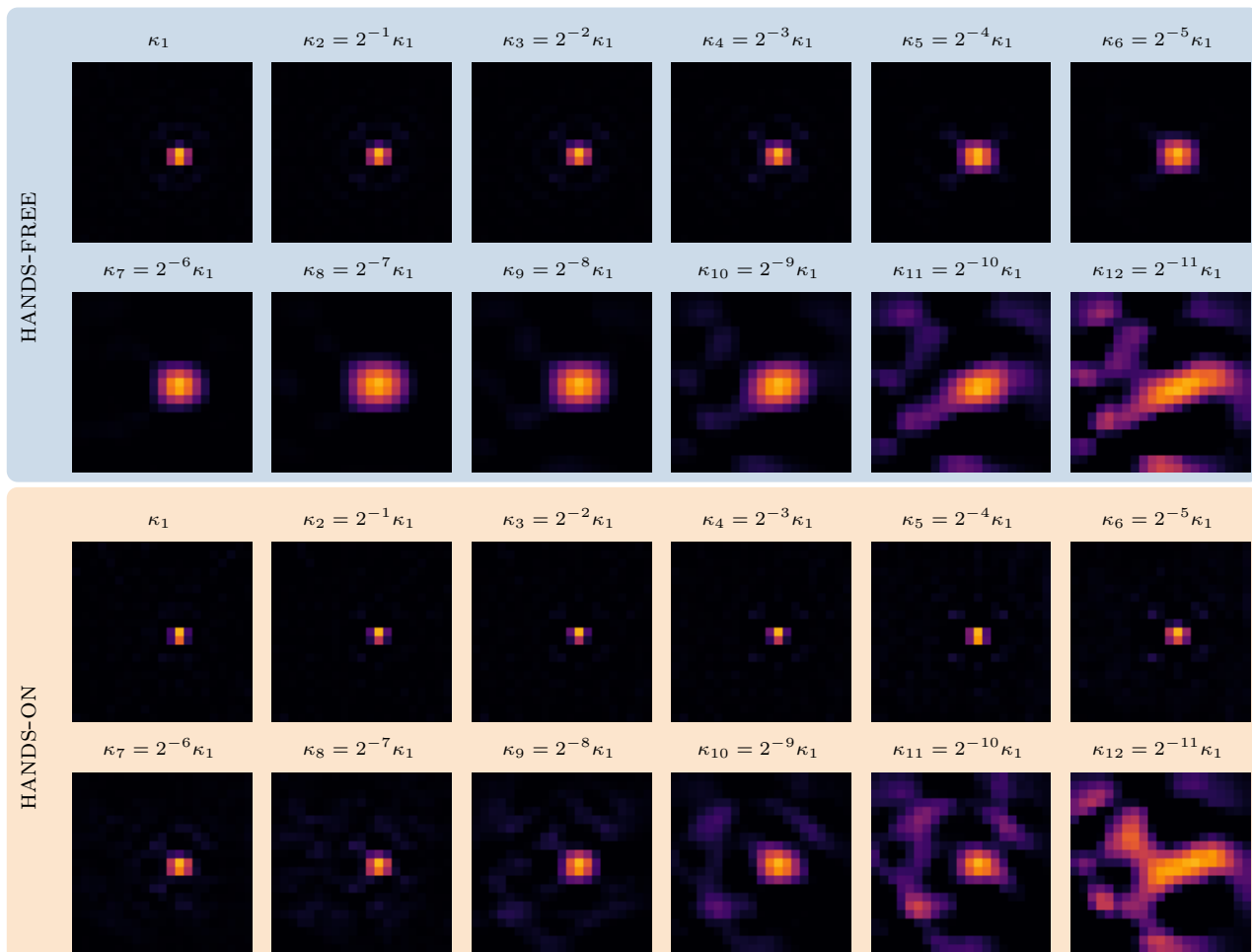


Figure 1: Reconstruction results for the hands-free method (top) and the optimal parameter set resulting from the grid search (bottom) for each concentration ($\kappa_1 = 400$ mmol/l). Shown is the xy -plane with a maximum intensity projection in z -direction.

of regularization over the different concentrations. Good results – both visually and with respect to the NRMSD – can be achieved over all concentrations. For the lowest two concentrations the results are even better than the best reconstruction result using hand-tuned parameters.

V. Discussion

The proposed method is able to find a reasonable compromise between resolution and noise and gives good reconstructions for MPI measurements with a broad band of iron concentrations. The results are not significantly worse than the reconstruction results using the optimal parameter set arising from an expensive tuning process by hand. For the lowest two concentrations, the hands-free reconstruction even gives a better NRMSD. The reason could be, that the changing of the reconstruction parameters between the first and second iteration gives a higher flexibility for such low concentrations. Altogether, this enables good 'plug and play' reconstructions without experience and prior knowledge on the data. Other

potential use-cases are measurements with a time dependent concentration, e.g. in vivo bolus measurements. To underline the power of the presented hands-free reconstruction, the method needs to be verified on various MPI data in future work. Another important step for future work on this topic is the derivation of the scanner-dependent tuning parameters α_Θ and Θ_{\min} directly from the measurement data.

VI. Conclusion

In this work we presented a method that is able to achieve good reconstruction results on MPI data with a very broad band of iron concentrations without any user input. This enables good 'plug and play' reconstruction results independent of the noise level and the iron concentration.

Acknowledgments

Research funding: The author state no funding involved.

Author's statement

Conflict of interest: Authors state no conflict of interest.

References

- [1] B. Gleich and J. Weizenecker. Tomographic imaging using the non-linear response of magnetic particles. *Nature*, 435(7046):1214–1217, 2005, doi:[10.1038/nature03808](https://doi.org/10.1038/nature03808).
- [2] T. Knopp, N. Gdaniec, and M. Möddel. Magnetic particle imaging: From proof of principle to preclinical applications. *Physics in Medicine and Biology*, 62(14):R124, 2017, doi:[10.1088/1361-6560/aa6c99](https://doi.org/10.1088/1361-6560/aa6c99).
- [3] T. Knopp, J. Rahmer, T. F. Sattel, S. Biederer, J. Weizenecker, B. Gleich, J. Borgert, and T. M. Buzug. Weighted iterative reconstruction for magnetic particle imaging. *Physics in Medicine and Biology*, 55(6):1577–1589, 2010, doi:[10.1088/0031-9155/55/6/003](https://doi.org/10.1088/0031-9155/55/6/003).
- [4] M. Boberg, N. Gdaniec, P. Szwargulski, F. Werner, M. Möddel, and T. Knopp. Simultaneous imaging of widely differing particle concentrations in MPI: Problem statement and algorithmic proposal for improvement. *Physics in Medicine and Biology*, 66(9), 2021, doi:[10.1088/1361-6560/abf202](https://doi.org/10.1088/1361-6560/abf202).
- [5] T. Knopp, S. Biederer, T. Sattel, and T. M. Buzug. Singular value analysis for magnetic particle imaging, in *2008 IEEE Nuclear Science Symposium Conference Record*, 4525–4529, 2008. doi:[10.1109/NSSMIC.2008.4774296](https://doi.org/10.1109/NSSMIC.2008.4774296).
- [6] H. Volkens, Y. Blancke Soares, T. Buzug, and K. Gräfe. Algorithm for computing optimal SNR thresholds of a single-sided FFP MPI device, 1, 8, 2022. doi:[10.18416/IJMPI.2022.2203043](https://doi.org/10.18416/IJMPI.2022.2203043).
- [7] J. Rahmer, J. Weizenecker, B. Gleich, and J. Borgert. Analysis of a 3-D system function measured for magnetic particle imaging. *IEEE Transactions on Medical Imaging*, 31(6):1289–1299, 2012, doi:[10.1109/TMI.2012.2188639](https://doi.org/10.1109/TMI.2012.2188639).